LARGE DEFLECTION OF CANTILEVER FUNCTIONALLY GRADED SANDWICH BEAM UNDER END FORCES BASED ON A TOTAL LAGRANGE FORMULATION

Bui Thi Thu Hoai[1, 2], Tran Thi Thu Huong[3], Nguyen Dinh Kien[1, 2, *], Vu Thi An Ninh[4]

[1]*Institute of Mechanics, VAST, 18 Hoang Quoc Viet, Ha Noi, Viet Nam*

[2]*Graduate University of Science and Technology, VAST, 18 Hoang Quoc Viet, Ha Noi, Viet Nam*

[3]*Phenikaa University, To Huu Street, Yen Nghia Ward, Ha Dong District, Ha Noi, Viet Nam*

[4]*University of Transport and Communications, 3 Cau Giay, Dong Da, Ha Noi, Viet Nam*

[*]Email: *ndkien@imech.vast.vn*

Abstract. A two-node beam element for large deflection analysis of cantilever functionally graded sandwich (FGSW) beams subjected to end forces is formulated in the context of total Lagrange formulation. The beams consist of three layers, a homogeneous core and two functionally graded layers with material properties varying in the thickness direction by a power gradation law. Linear functions are adopted to interpolate the displacement field and reduced integral technique is applied to evaluate the element formulation. Newton-Raphson based iterative algorithm is employed in combination with arc-length control method to compute equilibrium paths of the beams. Numerical investigations are given for the beam under a transverse point load and a moment to show the accuracy of the element and to illustrate the effects of material inhomogeneity and the layer thickness ratio on the large deflection behavior of the FGSW beams.

Keywords: Cantilever FGSW beam, large deflection, total Lagrange formulation, reduced integration, nonlinear beam element.

Classification numbers: 2.9.4, 5.4.2, 5.4.3.

1. INTRODUCTION

Large displacement analysis of beams and frames made of functionally graded materials (FGMs) is important in engineering design, and has drawn much attention from researchers in recent years. Based on a total Lagrange Timoshenko beam element, Kocatürk *et al.* [1] studied large displacement behavior of FGM beams due to distributed load. Based on a total Lagrange formulation, Almeida *et al.* [2] investigated geometrically nonlinear behavior of FGM beams subjected to end forces. Nguyen [3, 4], Nguyen and Gan [5] derived the co-rotational finite beam elements for studying large deflections of tapered FGM beams. The material properties of the beams are considered by the authors to vary in the beam thickness or length direction by a power

gradation law. The large deflections of FGM beams and frames were also considered by Nguyen *et al.* [6] using a co-rotational Euler-Bernoulli beam element. More recently, the effect of plastic deformation on post-buckling and nonlinear behavior of FGM beams [7, 8] were investigated by using the finite element method.

Sandwich structures with high strength-to-weight ratio are widely used in aerospace application such as skin of wings, aileron, and spoilers. In order to improve the performance of this type of structures, FGMs could be incorporated in the sandwich construction. Several analyses, mainly the vibration and buckling, of functionally graded sandwich (FGSW) beams have been carried out in recent years [9-11]. To maintain minimum weight for a given mechanical loading condition, FGSW beams and frames are often designed to be slender and they might undergo large displacements during service. Investigation on the large displacement behaviour of FGSW beams have been reported recently. In this line of work, Nguyen and Tran [12] derived a nonlinear beam element for investigating the large displacement behavior of FGSW beams and frames formed from a homogeneous metal core and two FGM face sheets.

The objective of this paper is to formulate a total Lagrange nonlinear beam element for studying large deflection behavior of cantilever FGSW beams under end forces. The beams considered herein consist of three layers, a homogeneous core and two FGM skin layers with power-law thickness variation of the material properties. Linear functions are used to interpolate the displacement field and reduced integral technique is applied to evaluate the element formulation to avoid the shear locking. Newton-Raphson based iterative algorithm is employed in combination with arc-length control method to compute equilibrium paths of the beams. Numerical investigations are carried out for the beam under a transverse point load and a moment. The effects of material inhomogeneity and the layer thickness ratio on the large deflection behavior of the beams are examined and highlighted.

2. FGM SANDWICH BEAM

Figure 1 shows an FGSW beam with length L and rectangular cross section $(b \times h)$ in a Cartesian coordinate system (x, z). The beam is composed from three layers, a homogeneous isotropic core and two FGM skin layers. In the figure, the Cartesian coordinate system (x, z) is chosen such that the x-axis is on the mid-plane, while the $z-$axis directs upward. Denoting $z_0, z_1, z_2 \ and \ z_3$ are, respectively, the vertical coordinates of the bottom surface, two interfaces between the layers and the top surface.
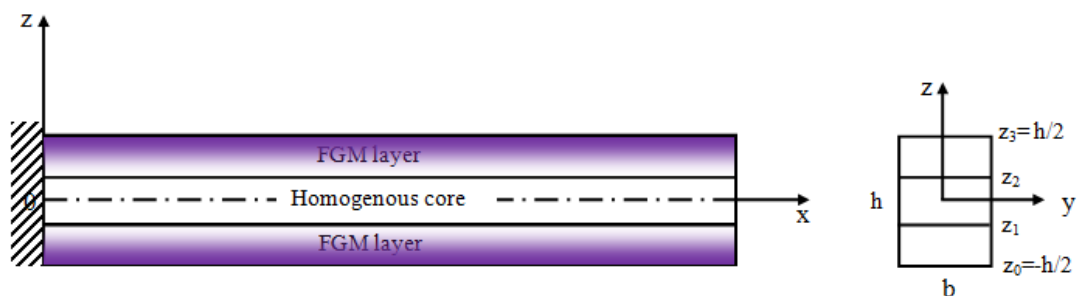

Figure 1. Geometry and coordinates of an FGSW beam.

The beam is assumed to be formed from two constituent materials, M1 and M2, in which the volume fraction $V_1^{(i)}$ $(i = 1, 2, 3)$ of M1 in the ith layer varies in the thickness direction according to

$$\begin{cases} V_1^{(1)} = \left(\dfrac{z - z_0}{z_1 - z_0} \right)^n, & \text{for } z \in [z_0, z_1] \\[2mm] V_1^{(2)} = 1, & \text{for } z \in [z_1, z_2] \\[2mm] V_1^{(3)} = \left(\dfrac{z - z_3}{z_2 - z_3} \right)^n, & \text{for } z \in [z_2, z_3] \end{cases} \tag{0}$$

and $V_2^{(i)} = 1 - V_1^{(i)}$. Mori-Tanaka scheme is employed herein to evaluate the effective properties of the FGM layers. In the scheme, the effective bulk modulus $\left(K_e^i \right)$ and shear modulus $\left(G_e^i \right)$ of the ith layer are given by

$$\frac{K_e^{(i)} - K_2}{K_1 - K_2} = \frac{V_1^{(i)}}{1 + V_2^{(i)} \left(K_1^{(i)} - K_2^{(i)} \right) / \left(K_2^{(i)} + 4G_2^{(i)}/3 \right)} \tag{2}$$

$$\frac{G_e^{(i)} - G_2^{(i)}}{G_1 - G_2} = \frac{V_1^{(i)}}{1 + V_2^{(i)} \left(G_1^{(i)} - G_2^{(i)} \right) / \left[G_2^{(i)} + G_2^{(i)} \left(9K_2^{(i)} + 8G_2^{(i)} \right) / \left(6K_2^{(i)} + 12G_2^{(i)} \right) \right]} \tag{3}$$

where K_1, K_2, G_1, G_2 are the bulk and shear moduli of M1 and M2. The effective Young's modulus E_f^i and Poisson's ratio v_f^i can be expressed as

$$E_f^{(i)} = \frac{9K_f^{(i)} G_f^{(i)}}{3K_f^{(i)} + G_f^{(i)}}, \quad v_f^{(i)} = \frac{3K_f^{(i)} - 2G_f^{(i)}}{6K_f^{(i)} + 2G_f^{(i)}}. \tag{4}$$

3. FINITE ELEMENT FORMULATION

A two-node beam element (i, j) with length of l is considered in this section. The vector of nodal displacements for an element with three degrees of freedom is

$$\mathbf{d} = \left\{ u_i \quad w_i \quad \theta_i \quad u_j \quad w_j \quad \theta_j \right\}^T \tag{5}$$

where u_i, w_i and θ_i are, respectively, the axial, transverse displacements and rotation at node i; u_j, w_j and θ_j are the corresponding quantities at node j.

The deformation at a point on the beam is defined by an angle θ, the rotation of its associated cross section, and a position vector as [13]

$$\mathbf{r}(x) = \{x + u(x)\} \mathbf{t}_1 + w(x) \mathbf{t}_2 \tag{6}$$

where $\mathbf{t}_1$, $\mathbf{t}_2$ are the base unit vectors; $0 \le x \le l$ is measured on the straight configuration; $u(x)$ and $w(x)$ are the axial and transverse displacement, respectively. The strain energy for the

beam element is given by

$$U = \frac{1}{2}\int_V \left[E(z)\varepsilon^2 + \psi G(z)\gamma^2 \right] dV = \frac{1}{2}\int_0^l \int_A \left[E(z)\varepsilon^2 + \psi G(z)\gamma^2 \right] dV \tag{7}$$

where V and A are the element volume and cross-sectional area; ψ is the shear correction factor, equal to $5/6$ for the rectangular section; ε and γ are the axial and shear strains

$$\varepsilon = \frac{\partial u}{\partial x} - z\frac{\partial \theta}{\partial x}, \quad \gamma = \frac{\partial w}{\partial x} - \theta \tag{8}$$

Using Eq. (7), we can write the strain energy in the form

$$U = \frac{1}{2}\int_V \left(A_{11}\varepsilon_0^2 + 2A_{12}\varepsilon_0\gamma + A_{22}\chi^2 + \psi A_{33}\gamma^2 \right) dx \tag{9}$$

with $\varepsilon_0 = \partial u / \partial x$ and $\chi = -\partial \theta / \partial x$ are the membrane strain and curvature, respectively; A_{11}, A_{12}, A_{22} and A_{33} are the rigidities, defined as

$$\left(A_{11}, A_{12}, A_{22} \right) = \sum_{i=1}^{3}\int_A E(z)\left(1, z, z^2 \right)dA, \quad A_{33} = \sum_{i=1}^{3}\int_A G(z)dA \tag{10}$$

where A denote the cross-sectional area.

It should be noted that for the large displacement considered herein, the strains ε_0, γ and the curvature χ, although parameterized for convenience by the reference abscissa x, take the values in the current configuration, and can be defined through the position vector in accordance with [13] as

$$\frac{\partial \mathbf{r}}{\partial x} = \left(1 + \varepsilon_0 \right)\mathbf{e}_1 + \gamma\mathbf{e}_2, \quad \chi = -\frac{\partial \theta}{\partial x} \tag{11}$$

where

$$\mathbf{e}_1 = \cos\theta\mathbf{t}_1 + \sin\theta\mathbf{t}_2, \quad \mathbf{e}_2 = \sin\theta\mathbf{t}_1 + \cos\theta\mathbf{t}_2 \tag{12}$$

are the unit vectors, parallel and orthogonal to the tangent of the beam axis. From Eqs. (5), (10) and (11), the membrane and shear strains can be written in the forms

$$\begin{cases} \varepsilon_o = \left(1 + \dfrac{\partial u}{\partial x} \right)\cos\theta + \dfrac{\partial w}{\partial x}\sin\theta - 1 \\[3mm] \gamma = -\left(1 + \dfrac{\partial u}{\partial x} \right)\sin\theta + \dfrac{\partial w}{\partial x}\cos\theta \\[3mm] \chi = -\dfrac{\partial \theta}{\partial x} \end{cases} \tag{13}$$

As the shear deformation is taken into account, the transverse displacement, $w(x)$ and the rotation, $\theta(x)$, are independent parameters, and linear functions can be employed to the interpolate displacements and rotation as

$$u = \frac{l-x}{l}u_i + \frac{x}{l}u_j, \; w = \frac{l-x}{l}w_i + \frac{x}{l}w_j, \; \theta = \frac{l-x}{l}\theta_i + \frac{x}{l}\theta_j \tag{14}$$

The beam element based on the shape function (13) does, however, encounter the shear-

locking problem, and to overcome this problem, the reduced integral, namely the one-point Gauss quadrature, is used herein to evaluate the strain energy of the beam element. In this context, one can write the strain energy in Eq. (8) in the form

$$U = \frac{l}{2}\left(A_{11}\bar{\varepsilon}_0^2 + 2A_{12}\bar{\varepsilon}_0\bar{\chi} + A_{22}\bar{\chi}^2 + \psi A_{33}\bar{\gamma}^2\right) \tag{15}$$

where $\bar{\varepsilon}_0, \bar{\gamma}, \bar{\chi}$ are given by

$$\begin{cases} \bar{\varepsilon}_o = \left(1 + \dfrac{u_j - u_i}{l}\right)\cos\bar{\theta} + \dfrac{w_j - w_i}{l}\sin\bar{\theta} - 1 \\[3mm] \bar{\gamma} = -\left(1 + \dfrac{u_j - u_i}{l}\right)\sin\bar{\theta} + \dfrac{w_j - w_i}{l}\cos\bar{\theta} \\[3mm] \bar{\chi} = \dfrac{\theta_j - \theta_i}{l}, \qquad\qquad \text{with} \qquad \bar{\theta} = \dfrac{\theta_i + \theta_j}{2} \end{cases} \tag{16}$$

With the above expression of the strain energy, one can compute the nodal internal force vector, $\mathbf{f}_{in}$ and the tangent stiffness, $\mathbf{k}_t$, for the element can be obtained by once and twice differentiating the strain energy with respect to the nodal displacement, respectively

$$\mathbf{f}_{in} = \frac{\partial U}{\partial \mathbf{d}} = \mathbf{f}_a + \mathbf{f}_c + \mathbf{f}_b + \mathbf{f}_s \tag{17}$$

$$\mathbf{k}_t = \frac{\partial^2 U}{\partial \mathbf{d}^2} = \mathbf{k}_a + \mathbf{k}_c + \mathbf{k}_b + \mathbf{k}_s$$

where the subscripts a, c, b, s denote the terms stemming from the axial stretching, axial-bending coupling, bending and shear deformation of the beam, respectively.

In the large displacement analysis, both the internal force vector $\mathbf{f}_{in}$ and the tangent stiffness matrix $\mathbf{k}_t$ depend on the current nodal displacements $\mathbf{d}$. The detailed expressions for the internal force vector and tangent stiffness matrix in Eq. (16) are given in the Appendix.

4. EQUILIBRIUM EQUATION

The equilibrium equation for the beam can be written in the form

$$\mathbf{g}(\mathbf{p}, \lambda) = \mathbf{q}_{in}(\mathbf{p}) - \lambda\mathbf{f}_{ex} = \mathbf{0} \tag{18}$$

where the residual force vector $\mathbf{g}$ is a function of the current structural nodal displacements $\mathbf{p}$, and the load level parameter λ; $\mathbf{q}_{in}$ is the structural nodal force vector, assembled from the formulated vector $\mathbf{f}_{in}$; $\mathbf{f}_{ex}$ is the fixed external loading vector.

The Newton-Raphson based iterative procedure is used in combination with arc-length control technique herein to solve the nonlinear equation (17). The detail of this method is described in [14].

5. NUMMERICAL RESULTS AND DISCUSSIONS

An FGSW beam made of Aluminum (Al) and Zirconia (ZrO_2), with core is pure ZrO_2, subjected to a transverse load P at its free end is firstly considered. Young's modulus of Al is 70 GPa and that of ZrO_2 is 151 GPa. An aspect ratio $L/h = 50$ is assumed for the beam. In order to facilitate discussion of the numerical results, the following dimensionless parameter is introduced as

$$w^* = \frac{w_L}{L} \tag{19}$$

where w_L denotes the vertical displacement at the free end of the beam.

Table 1. Comparison of normalized tip deflections, $w(L)/L$, of isotropic beam under transverse tip load.

$PL^2/E_m I$	Mattiasson [15]	Nguyen and Tran [12]	Present
1	0.30172	0.30172	0.2981
2	0.49346	0.49349	0.4898
3	0.60325	0.60331	0.6003
4	0.66996	0.67004	0.6676
5	0.71379	0.7139	0.7117
6	0.74457	0.7447	0.7426
7	0.76737	0.76753	0.7654
8	0.78498	0.78517	0.7829
9	0.79906	0.79926	0.7969
10	0.81061	0.81085	0.8084

Table 2. Normalized tip deflection, $w(L)/L$, of FGSW beam under transverse load.

$PL^2/E_m I$	n	(1-0-1)	(8-1-8)	(2-1-2)	(1-1-1)	(2-2-1)	(1-2-1)
5	0.5	0.6386	0.6359	0.6282	0.6187	0.6138	0.6036
	1	0.6732	0.6704	0.6704	0.6504	0.6416	0.6310
	5	0.7091	0.7080	0.7031	0.6937	0.6807	0.6727
10	0.5	0.7659	0.7642	0.7596	0.7539	0.7512	0.7446
	1	0.7861	0.7845	0.7795	0.7728	0.7679	0.7613
	5	0.8068	0.8062	0.8034	0.7980	0.7908	0.7858

The validation of the derived formulation is needed to confirm. In Table 1, the normalized tip deflection of the isotropic cantilever beam obtained in the present work is compared to the analytical solution of Mattiasson [15] and the finite element result of Nguyen and Tran [12]. In the table (and following also), E_m denotes Young's modulus of the metal (Al). Very good agreement between the result of the present work with that of Refs. [12, 15] is noted from Table 1. Noting that the result in Table is converged.

Table 2 lists the normalized tip deflection, $w(L)/L$, of the cantilever FGSW beam under transverse tip load for two value of the applied load and various values of the material index and the layer thickness ratio. In the table and hereafter, three numbers in the brackets are used herein

to denote the layer thickness ratio, e.g. (2-1-1) means that $(h_1 : h_2 : h_3) = $ (2-1-1). The effects of the material index n and the layer thickness ratio on the deflection of the beam are clearly seen from the table. The deflection is smaller for the beam with a larger core thickness, and it is larger for the beam associated with a higher index *n*. The increase of the deflection can be explained by the fact that, the beam associated with a higher index *n* contains less ceramic. Since Young's modulus of the ceramic is considerable higher than that of the metal, the rigidities of the beam with less ceramic percentage are smaller, and this leads to the larger deflection. On the other hand, the beam with larger core thickness contains more ceramic percentage and thus has higher rigidities, and this leads to a lower deflection.
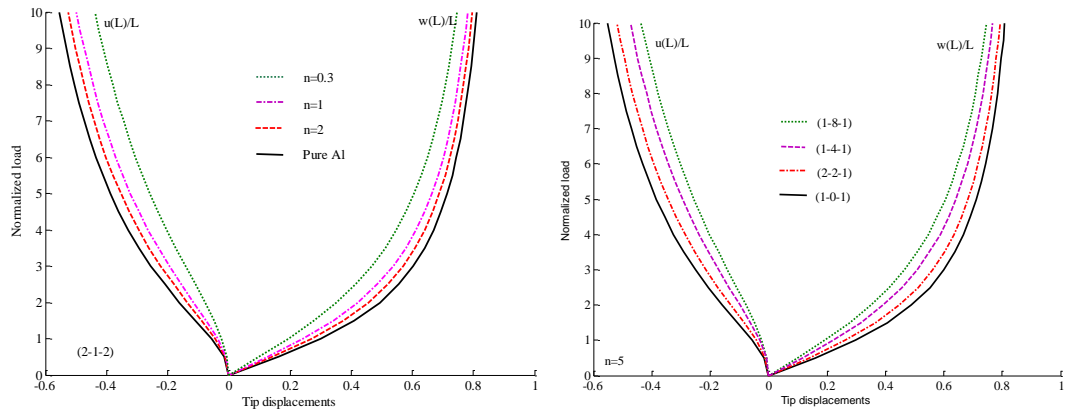
Figure 2. Effect of grading index n (left) and layer thickness ratio (right) on the tip response of FGSW beam under transverse tip load.
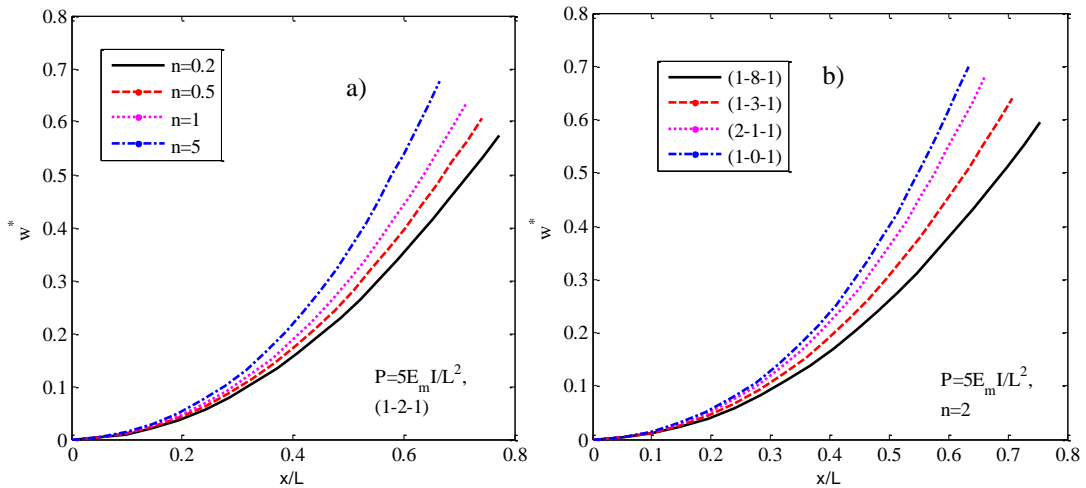
Figure 3. Deformed configurations of FGSW cantilever beam under transverse tip load.

The effect of the grading index *n* and the layer thickness ratio on the large displacement response of the FGSW cantilever beam can also be seen from Figure 2, where the load-displacement curves of the FGSW beam are shown for various values of the index *n* and the layer thickness ratio. At a given value of the applied load, the tip displacements increase as the

grading index increases. The increase of the displacements, as explained above, is resulted from the lower rigidities of the beam associated with a higher index n. The tip displacements of the beam are increased by the decrease of the core thickness, regardless of the load level. The deformed configurations of the beam as depicted in Figure 3 for two values of the applied load, $P = 5E_m I / L^2$ and $P = 10E_m I / L^2$, also confirm the effects of the material distribution and the layer thickness ratio on the large displacement response of the FGSW beam. The configurations shown in the figures have been computed by using sixteen elements in order to ensure the smoothness of the curves.
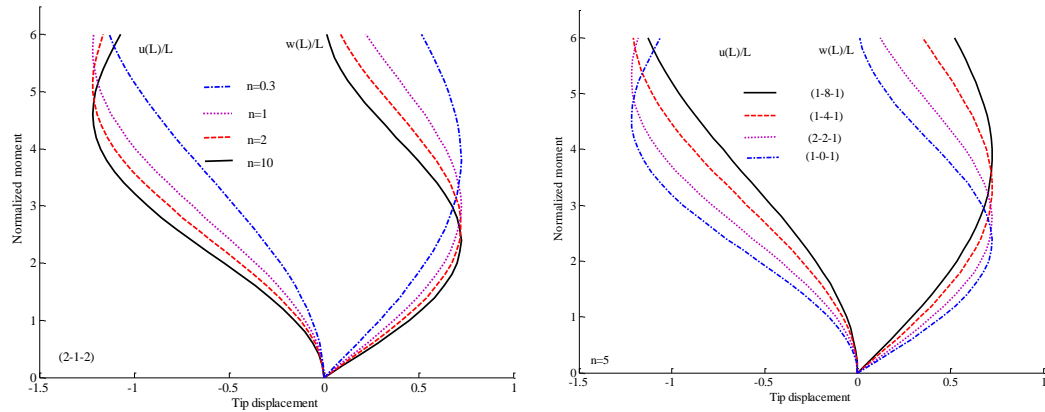
Figure 4. Tip displacement response versus tip moment of FGSW cantilever beam.
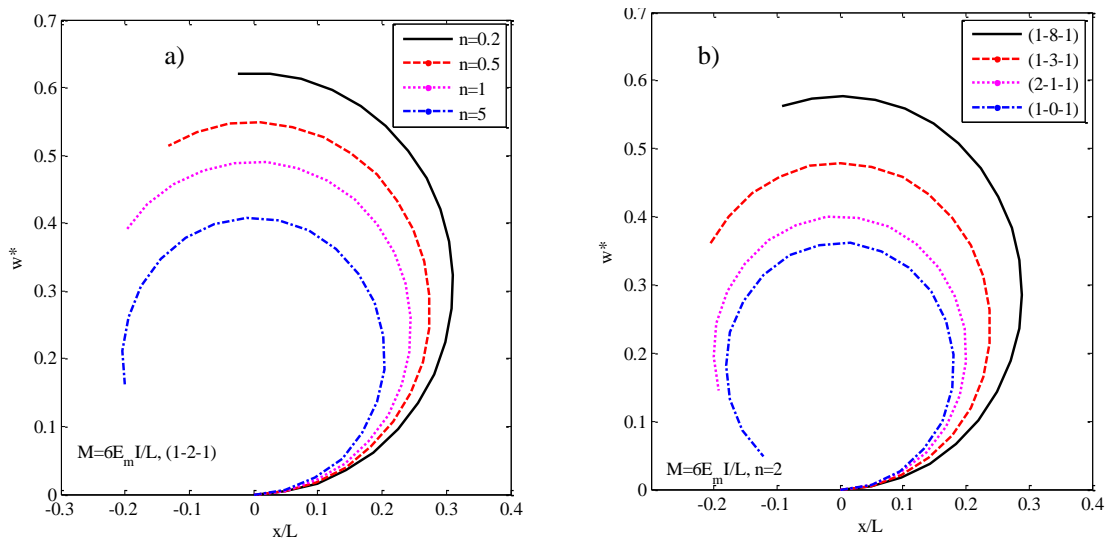
Figure 5. Deformed configurations of FGSW cantilever beam subjected to a tip moment.

Next, a cantilever FGSW subjected to a tip moment M is analyzed. In Figure 4 and Figure 5 show the load-displacement curves and the deformed configuration of the beam for various values of the material grading index *n* and different layer thickness ratio. The influence of the material distribution and the layer thickness ratio on the response of the beam is also clearly from the figures. Noting that the arc-length control technique must be employed to trace the snap-back in the load-displacement curves in Figure 3.

6. CONCLUSIONS

A nonlinear beam element for large displacement of an FGSW beam has been formulated and employed in computing the response of a cantilever beam subjected to a transverse load and a moment at its free end. The beam is considered to beam formed from three layers, a homogeneous cure and two FGM skin layers. The effective material properties of functionally graded materials are assumed to vary continuously in the thickness direction by a power-law distribution in terms of volume fraction of constituents, and they are estimated by Mori-Tanaka scheme. Based on the total Lagrange formulation, the internal force vector and tangent stiffness matrix for the element are computed from the strain energy expression Reduced integration method was adopted to overcome the shear locking of the derived formulation. The numerical results have shown the accuracy of the present method. A parametric study has been carried out to show the influence of material inhomogeneity and the layer thickness ratio on the large deflection behavior of the beams.

REFERENCES

1. Kocatürk M., Simsek M., and Akbas S. D. - Large displacement static analysis of a cantilever timoshenko beam composed of functionally graded material, Science Engineering Composite Materials **18** (2011) 21-34.

2. Almeida C. A., Albino J. C. R., Menezes I. F. M., Paulino G. H. - Geometric nonlinear analyses of functionally graded beams using a tailored Lagrangian formulation, Mechanics Research Communications **38** (2011) 553-559.

3. Nguyen D. K. - Large displacement response of tapered cantilever beams made of axially functionally graded material, Compos Part B-Eng. **55** (2013) 298-305.

4. Nguyen D. K. - Large displacement behaviour of tapered cantilever Euler-Bernoulli beams made of functionally graded material, Applied Mathematic and Computation **237** (2014) 340-55.

5. Nguyen D. K., Gan B. S. - Large deflections of tapered functionally graded beams subjected to end forces, Applied Mathematical Modelling **38** (2014) 3054-66.

6. Nguyen D. K., Gan B.S., Trinh T. H. - Geometrically nonlinear analysis of planar beam and frame structures made of functionally graded material, Structural Engineering and Mechanics **49** (2014) 727-743.

7. Trinh T. H., Nguyen D. K., Gan B. S., Alexandrov S. - Post-buckling responses of elastoplastic FGM beams on nonlinear elastic foundation, Structural Engineering and Mechanics **58** (2016) 515-32.

8. Nguyen D. K., Nguyen K. V., Dinh V. M., Gan B. S., Alexandrov S. - Nonlinear bending of elastoplastic functionally graded ceramic-metal beams subjected to nonuniform distributed loads, Applied Mathematics and Computation **333** (2018) 443-59.

9. Bui Q. T., Khosravifard A., Zhang Ch., Hematiyan M. R., and Golub M. V. -Dynamic analysis of sandwich beams with functionally graded core using a truly meshfree radial point interpolation method, Engineering Structures **47** (2013) 90–104.

10. Vo T. P., Thai H. T., Nguyen T. K., Maheri A., and Lee J. - Finite element model for vibration and buckling of functionally graded sandwich beams based on a refined shear deformation theory, Engineering Structures **64** (2014) 12–22.

11. Vo T. P., Thai H. T., Nguyen T. K., Inam F., and Lee J. - A quasi-3D theory for vibration and buckling of functionally graded sandwich beams, Composite Structures **119** (2015) 1–12.

12. Nguyen D. K., Tran T. T. - A corotational formulation for large displacement analysis of functionally graded beam and frame structures, Mathematical Problems in Engineering (2016) http://dx.doi.org/10.1155/2016/5698351

13. Nguyen D. K. - Post-buckling behavior of beams on two-parameter elastic foundation, International Journal of Structural Stability and Dynamics **4** (1) (2014) 21-43.

14. Crisfiled M. A. - Nonlinear Finite Element Analysis of Solids and Structures, volume 1: Essential, John Wiley & Sons, Chichester, 1991.

15. Mattiasson K. - Numerical results from large deflection beam and frame problems analysed by means of elliptic integrals, International Journal for Numerical Methods in Engineering **17** (1) (1981) 145–153.

APPENDIX

Detail expresstion for the nodal forces and the tangent stiffness matrices in Eq. (16) are as follows

$$\mathbf{f}_a = A_{11}\bar{\varepsilon}_0 \left\{ -c \quad -s \quad \frac{l}{2}\bar{\gamma} \quad c \quad s \quad \frac{l}{2}\bar{\gamma} \right\}^T \; ; \; \mathbf{f}_b = A_{22}\bar{\kappa} \{0 \;\; 0 \;\; 1 \;\; 0 \;\; 0 \;\; -1\}^T \; ;$$

$$\mathbf{f}_c = A_{12}\bar{\varepsilon}_0 \{0 \;\; 0 \;\; 1 \;\; 0 \;\; 0 \;\; -1\}^T + A_{12}\bar{\kappa} \left\{ -c \quad -s \quad \frac{l}{2}\bar{\gamma} \quad c \quad s \quad \frac{l}{2}\bar{\gamma} \right\}^T \; ;$$

$$\mathbf{f}_s = \psi A_{33}\bar{\gamma} \left\{ s \quad -c \quad -\frac{l}{2}(1+\bar{\varepsilon}) \quad -s \quad c \quad -\frac{l}{2}(1+\bar{\varepsilon}) \right\}^T \; ;$$

$$\mathbf{k}_a = \frac{1}{l}A_{11} \begin{bmatrix} c^2 & & & & & \\ sc & s^2 & & & sym. & \\ \frac{l}{2}a_1 & -\frac{l}{2}a_2 & \frac{l^2}{4}a_3 & & & \\ -c^2 & -sc & -\frac{l}{2}a_1 & c^2 & & \\ -sc & -s^2 & \frac{l}{2}a_5 & sc & s^2 & \\ \frac{l}{2}a_1 & -\frac{l}{2}a_2 & \frac{l^2}{4}a_3 & -\frac{l}{2}a_1 & \frac{l}{2}a_2 & \frac{l^2}{4}a_3 \end{bmatrix} ;$$

$$\mathbf{k}_b = \frac{1}{l}A_{22} \begin{bmatrix} 0 & & & & & \\ 0 & 0 & & & sym. & \\ 0 & 0 & 1 & & & \\ 0 & 0 & 0 & 0 & & \\ 0 & 0 & 0 & 0 & 0 & \\ 0 & 0 & -1 & 0 & 0 & 1 \end{bmatrix} ;$$

$\mathbf{k}_c =$

$$A_{12}\overline{\kappa}\begin{bmatrix} 0 & 0 & s & 0 & 0 & s \\ 0 & 0 & -c & 0 & 0 & -c \\ \dfrac{1}{2}s & -\dfrac{1}{2}c & -\dfrac{l}{2}(1+\overline{\varepsilon}) & -\dfrac{1}{2}s & \dfrac{1}{2}c & \dfrac{l}{2}(1+\overline{\varepsilon}) \\ 0 & 0 & -s & 0 & 0 & -s \\ 0 & 0 & c & 0 & 0 & c \\ \dfrac{1}{2}s & -\dfrac{1}{2}c & -\dfrac{l}{2}(1+\overline{\varepsilon}) & -\dfrac{1}{2}s & \dfrac{1}{2}c & \dfrac{l}{2}(1+\overline{\varepsilon}) \end{bmatrix}$$

$$+\frac{2}{l}A_{12}\begin{bmatrix} 0 & 0 & -c & 0 & 0 & c \\ 0 & 0 & -s & 0 & 0 & s \\ 0 & 0 & \dfrac{l}{2}\overline{\gamma} & 0 & 0 & -\dfrac{l}{2}\overline{\gamma} \\ 0 & 0 & c & 0 & 0 & -c \\ 0 & 0 & s & 0 & 0 & -s \\ 0 & 0 & \dfrac{l}{2}\overline{\gamma} & 0 & 0 & -\dfrac{l}{2}\overline{\gamma} \end{bmatrix} \quad ;$$

$\mathbf{k}_s =$

$$\frac{\psi}{l}A_{33}\begin{bmatrix} s^2 & & & & & \\ -sc & c^2 & & & & \\ -s^2 & \dfrac{l}{2}a_5 & \dfrac{l^2}{4}a_6 & & & \\ -s^2 & sc & -\dfrac{l}{2}a_4 & s^2 & & \\ sc & -c^2 & -\dfrac{l}{2}a_5 & -sc & c^2 & \\ \dfrac{l}{2}a_4 & \dfrac{l}{2}a_5 & \dfrac{l^2}{4}a_6 & -\dfrac{l}{2}a_4 & -\dfrac{l}{2}a_5 & \dfrac{l^2}{4}a_6 \end{bmatrix} \quad ;$$

where

$$s = \sin\overline{\theta}; \qquad\qquad c = \cos\overline{\theta};$$
$$a_1 = (s\overline{\varepsilon} - c\overline{\gamma}); \qquad a_2 = (c\overline{\varepsilon} + s\overline{\gamma});$$
$$a_3 = \overline{\gamma}^2 - \overline{\varepsilon}(1+\overline{\varepsilon}); \quad a_4 = c\overline{\gamma} - s(1+\overline{\varepsilon});$$
$$a_5 = s\overline{\gamma} + c(1+\overline{\varepsilon}); \quad a_6 = (1+\overline{\varepsilon})^2 - \overline{\gamma}^2.$$

42